

## BUBBLE GROWTH IN A NARROW HORIZONTAL SPACE

Benoit Stutz, Remi Goulet\*, Julio Cesar Passos<sup>o</sup>

\* CETHIL, UMR5008, CNRS, INSA-Lyon, Université Lyon1, F69621 Villeurbanne, France,

<sup>o</sup> Departamento de Engenharia Mecânica, LABSOLAR-CNTS, Universidade Federal de Santa Catarina, Cx. P. 476  
88010-900 Florianópolis, S.C., Brasil

### ABSTRACT

The purpose of this work is to develop an axi-symmetric two-phase flow model describing the growth of a single bubble squeezed between a horizontal heated upward-facing disc and an insulating surface placed parallel to the heated surface.

Heat transfers at the liquid-vapour interfaces are predicted by the kinetic limit of vaporisation. The depths of the liquid films deposited on the surfaces (heated surface and confinement space) are determined using the Moriyama and Inoue correlation (1996). Transient heat transfers within the heated wall are taken into account. The model is applied to pentane bubble growth. The influence of the gap size, the initial temperature of the system, the thermal effusivity of the heated wall and the kinetic limit of vaporisation are studied.

The results show that the expansion of the bubbles strongly depends on the gap size and can be affected by the effusivity of the material. Mechanical inertia effects are mainly dominant at the beginning of the bubble expansion. Pressure drop induced by viscous effects have to be taken into account for high capillary numbers. Heat transfers at the meniscus are negligible except at the early stages of the bubble growth.

### INTRODUCTION

Most of the production costs of consumer products are directly related to the amount of raw material involved in their manufacturing. Cost down lead to increase the compactness and thus the specific power of the systems. The thermal control devices involved in the systems requires more and more efficient cooling processes insuring increasing heat flux removing in reducing spaces. Boiling in narrow spaces is an attractive solution that can satisfied requirement. It enables to transfer heat flux up to  $10^5 \text{Wm}^{-2}$  between parallel plates characterised by confinement gap size smaller than 1 mm [1].

Compared with unconfined pool boiling, confinement improves heat transfer at low heat flux but reduces heat transfer at high heat flux. Researches on boiling in narrow horizontal spaces began in the 70' [2] [3] for saturated water at atmospheric pressure. It was found that heat transfer increases significantly at low heat flux when the gap size becomes smaller than the bubble detachment diameter. The preliminary results have been confirmed with different highly wetting fluids like FC72 [4] and FC87 [5], and pentane [1]. For subcooled conditions, the effect of the confinement is opposite to that for saturated boiling (an increase in the confinement cause a reduction in the heat transfer coefficient) [6]. In the same way, higher heat transfer coefficients for mixtures of binary water/ethylene-glycol than for pure water are observed in confined configurations because of the change in some fluid properties implying a decrease in the bubble diameter. The mass diffusion process and the increase of the fluid viscosity are considered as beneficial phenomenon to limit heat transfer deterioration at high heat flux.

Unsteady boiling occurs when a preference vapour evacuation direction exists, and when the gap size is closed to

the capillary length. The frequency of the unsteady boiling cycles depends on two characteristic times: the feeding time and the expansion time, the expansion time being the predominant time during the cycle [8].

Different correlations have been developed to describe heat transfer during natural circulation boiling of saturated liquids. None of them seems to be able to predict heat transfer when the conditions are significantly different from the one for which the correlation have been developed. This may be attributed to the fact that none of them properly takes into account the heat transfer mechanism : heat transfer enhancement is due to the evaporation of thin liquid films formed downstream liquid slug moving in the confined space (local heat transfer coefficient is then typically on the order of several times that of the liquid slug).

The presence of the evaporating film located between the squeezed bubble and the walls has been pointed out using an interferometer device [9]. The thickness of the liquid film  $\delta_0$  at the base of the travelling meniscus has been estimated by using an inverse heat conduction method for bubbles growing between two horizontal discs [10]. It depends on the gap size, the displacement velocity of the interfaces and the physical properties of the liquid. For low Bond numbers defined as the ratio of inertia forces to capillary forces ( $Bo^* = \frac{\rho s^2 U}{\sigma t_g}$ ),  $\delta_0$  is

controlled by the capillary number  $Ca = \frac{\mu \cdot U}{\sigma}$  :

$$Bo^* < 2 \Rightarrow \frac{\delta_0}{s} = 0.07 \cdot Ca^{0.41} \quad (1)$$

For high  $B_o^*$ ,  $\delta_0$  is controlled by the viscous sub-layer

$$\delta^* = \frac{\sqrt{V_l t_s}}{s}$$

$$Bo^* \geq 2 \Rightarrow \delta_0 = 0.1s \delta^{*0.84} \quad (2)$$

The most promising way to predict heat transfer in confined configuration seems to develop two-phase flow models describing the transient variation in local heat transfer coefficient during the passage of elongated bubbles. Thom et al [11] developed such a model for flow boiling in microchannels (three-zone model). The model shows the strong dependency of heat transfer on the bubble frequency, the minimum liquid film thickness at dryout and the liquid film formation thickness.

The purpose of this work is to develop an axi-symmetric two-phase flow model describing boiling between a horizontal heated upward-facing disc and an unheated surface placed parallel to the heated surface. This paper concerns the growth of a single bubble in the narrow horizontal space. The model is applied to pentane bubble growth. The influence of the gap size, the initial temperature of the system, the thermal effusivity of the heated wall and the kinetic limit of vaporisation are studied.

## HEAT TRANSFER MODEL

The model developed aims at giving an insight into the mechanisms controlling nucleate boiling heat transfer in a narrow gap formed by horizontal and parallel disks. A perfect case (Figure 1) lending itself easily to theoretical analysis is considered: a single bubble grows from a nucleation site located at the centre of the upward facing heated wall. The confinement wall constraints the bubble growth. The phenomenon under concern is assumed to be axisymmetric. Heat transfer in confined boiling is mainly controlled by liquid layers formed on the walls. Thin layers thickness and length depend on local phase change and bubble growth rate. Therefore, knowledge of instantaneous quantities such as meniscus location and velocity, wall temperature field and vapour pressure and temperature, is required to give a physical picture of the phenomena involved in the flattened bubble growth.

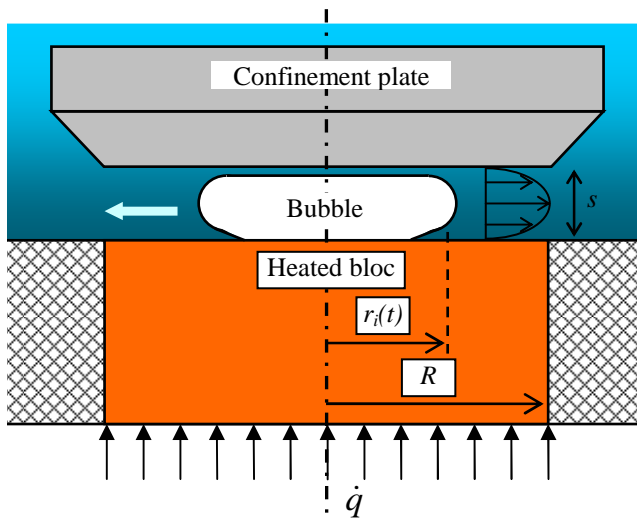


Fig. 1 :Geometry of the system.

## Model assumptions

The model is based on the following assumptions:

- 1) All phenomena taken into account are axisymmetric
- 2) Body forces are neglected
- 3) The heated block is insulated so that lateral heat losses are negligible
- 4) Thermodynamic equilibrium prevails in the vapour phase. Its behaviour is well described by ideal gas law
- 5) Velocity profile in the liquid phase is parabolic and described by a 2nd order polynomial
- 6) Heat flux transferred by convection in the liquid slug (upstream from the meniscus) and the vapour slug (dry zone) are negligible.
- 7) The confinement wall is adiabatic
- 8) The temperature of liquid vapour interfaces is equal to vapour temperature except at the inferior microfilm interface where an interfacial resistance is taken into account.

Heat and mass transfers at the liquid vapour interfaces are determined using the kinetic theory of gases. The theoretical net flow-rate of molecules that can leave an interface during vaporisation process or can be caught by the liquid phase during condensation process is limited. The amount of molecules that is really submitted to phase change can be determined from this theoretical limit using an accommodation coefficient  $\alpha$ . The maximum heat flux that can be transferred at the interface and thus the interfacial heat transfer coefficient at the interface  $h_{lim}$  is deduced from this coefficient (Carey ())

$$h_{lim} = \frac{2 \cdot \alpha}{2 - \alpha} \left( \frac{\Delta h_{lv}^2 \cdot \rho_v}{T_{sat} \cdot \mu_v} \right) \sqrt{\frac{\bar{M}}{2 \cdot \pi \cdot \bar{R} \cdot T_{sat}}} \left( 1 - \frac{P_{sat} \cdot \mu_v}{2 \cdot \Delta h_{lv} \cdot \rho_v} \right) \quad (3)$$

$h_{lim}$  is very high and interfacial resistance  $1/h_{lim}$  can be neglected most of the time (this comes to consider a imposed temperature condition at the interface) excepted when heat transfer catch up with the upper limit. In the present case, this limit can be reached in the vicinity of the triple line when the depth of the liquid film  $\delta(r,t)$  tends to zero and is submitted to heat flux.

Mass and momentum balances are applied to the liquid ring enclosed between the meniscus of the growing bubble and the external cylindrical surface of the confined space (the density ratio between the vapour and the liquid phases is negligible  $\rho_v/\rho_l \ll 1$  ; The amount of liquid trapped between the bubble and the walls is negligible ( $\delta \ll s$ )).

## Mass balance

Mass balance yields to the following equation:

$$r_i(t) \cdot \frac{\partial r_i}{\partial t} = R_0 \cdot \bar{u}(R_0, t) \quad (4)$$

Where  $r_i(t)$  and  $\bar{u}(R_0, t)$  are the instantaneous meniscus position and instantaneous liquid mean velocity at the domain external frontier, respectively.

## Momentum balance

Pressure difference between vapour and liquid outside the confined zone constitutes the driving force. The drag force acting on the liquid is easily calculated from assumption (5) and the no slip condition at the walls. The pressure drop through the meniscus involved by capillary action is deduced from the bubble curvature (meniscus is assumed to be a half torus) and the fluid surface tension. A singular pressure drop at the domain external frontier (section enlargement) is also taken into account.

Liquid ring momentum temporal variation is equal to the sum of forces acting on the fluid. The momentum equation radial component is simplified using Equation (1) which yields:

$$\rho_l \cdot (R - r_i(t)) \frac{d^2 r_i}{dt^2} = [P_{sat}(T_v(t)) - (P_{sat} + \rho_l \cdot g \cdot h)] - \frac{12}{s^2} \cdot \mu_l \cdot \frac{\partial r_i}{\partial t} \cdot (R - r_i(t)) + 0.5^2 \cdot \rho_l \cdot \left( \frac{r_i(t)}{R} \cdot \frac{\partial r_i}{\partial t} \right)^2 \frac{R}{r_i(t)} - \sigma \left( \frac{2}{s} + \frac{1}{r_i(t)} \right) - \frac{\rho_l (R - r_i(t))^2}{R r_i(t)} \left( \frac{\partial r_i}{\partial t} \right)^2 \quad (5)$$

This second order differential equation gives the bubble radius evolution.

### Energy balance

Vapour mass and pressure inside the bubble are deduced from the energy balances over the entire liquid vapour interface. Three different zones are considered: the lower liquid film deposited on the heated surface, the upper liquid film that covered the confinement plate and the lateral meniscus.

Vaporisation occurs on the lower film. The meniscus and the upper liquid film are submitted to condensation or vaporation depending on the temperature difference between the saturated vapour and the liquid.

The depth of the liquid films deposited at the base of the meniscus on the heated surface and on the confinement plate are determined using the correlation proposed by Moriyama et Inoue [10]

#### Phase change at the lower liquid film

The liquid film deposited on the heated surface is supposed to be stagnant. The liquid used (pentane) is a very highly wetting fluid (contact angle for 1 bar  $\theta < 5^\circ$ ). Liquid-vapour surface energy is not sufficient to break the liquid film and form droplets on the wall. Temperature at the interface is equal to the saturated temperature except in the closed vicinity of the triple line. Moreover the surface tension variation with temperature is very small ( $\Delta\sigma \approx 10^{-5} \text{ Nm}^{-1}\text{K}^{-1}$ ). Therefore Marangoni effects can not lead to liquid motion.

Let's have a look to the heat transfer within the liquid film deposited on the heated surface. The maximum depth of the liquid film deposited by the bubbles on the surfaces is  $\delta_{car} \approx 10 \mu\text{m}$ . The maximum heat flux that can be transferred at the interface during the vaporization process is about  $\dot{q}_{car} \approx 10^6 \text{ Wm}^{-2}$ . The characteristic time  $t_{car}$  needed to evaporate the liquid film in extreme conditions is about

$$t_{car} = \frac{\delta_{car} \rho_l \Delta h_{lv}}{\dot{q}_{car}} = 2.1 \cdot 10^{-4} \text{ s}.$$

The corresponding Fourier number of the heat transfer within the liquid film in such condition is about  $F_o = \frac{\lambda_l t_{car}}{\rho_l c_{pl} \delta_{car}^2} = 15$

Therefore it is reasonable to consider the thermal inertia negligible (heat transfers within the liquid film are controlled by conduction); Heat flux transferred from the wall to the liquid film is entirely used to vaporize the liquid. Thus, the film thickness evolution, at location  $r$ , during interval time  $dt$ , is given by:

$$\delta(r, t + dt) = \delta(r, t) - \frac{\dot{q}_{wall}(r, t) \times dt}{\Delta h_{lv} \times \rho_l} \quad (6)$$

The amount of vapour supplied by an axisymmetric surface element during  $dt$  is deduced from (3):

$$dm_{inf} = \rho_l \times 2 \times \pi \cdot r \cdot dr \times (\delta(r, t) - \delta(r, t + dt)) \quad (7)$$

#### Phase change at the meniscus

The interface is assumed to be at the vapour saturation temperature corresponding to the pressure inside the bubble. Liquid motion close to the meniscus is neglected. Heat flux transferred between the liquid and the vapour phase is determined from non stationary heat conduction problem inside the surrounding liquid.

Phase change is assumed to be uniform, therefore isotherms are concentric. The confinement width is about 1mm whereas the sample radius is equal to 15mm. Thus, as the bubble grows, the bubble curvature  $1/r$  decreases and rapidly and becomes much smaller than the meniscus curvature  $2/s$ . For convenience, the effect of bubble curvature is neglected which makes the heat conduction problem one-dimensional.

Moreover, meniscus is considered to be a half torus and the depth of the liquid films are not taken into account (Fig.2).

The amount of vapour vaporized or condensed during time  $dt$  is given by:

$$\dot{q}_{men} \cdot dt \cdot S_{men} = dm_{men} \cdot \Delta h_{lv} \quad (8)$$

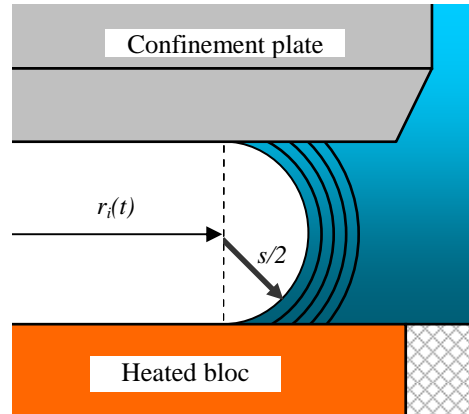


Fig.2: Bubble and meniscus radii

#### Phase change at the upper liquid film

As for the meniscus, evaporation or condensation occurs on the upper liquid film. The confinement wall is assumed to be adiabatic. Transient effects are negligible. Therefore, the film temperature is uniform and equal to interface temperature (which is equal to the saturation temperature, according to assumption 8).

At a given time, meniscus and inferior microfilm contribution to the vapour phase, during  $dt$ , is calculated (Equations (6) and (8)). New thermodynamic conditions in the bubble are deduced. The contribution of the superior microfilm is not yet taken into account; thus, the bubble is in a fictive state. An enthalpy balance over the fictive system constituted by the superior microfilm and the vapour enables to calculate the real thermodynamic conditions in the bubble at the final state, which yields the number of vapour moles produced by the superior microfilm during  $dt$ .

## Vapour temperature and vapour pressure in the bubble

The number of vapour moles  $n(t)$  inside the bubble is determined using energy balances. Considering the liquid-vapour interfacial area, the vapour phase inside the bubble is assumed to be in saturated conditions. The temperature and the pressure of the saturated vapour are determined using the ideal gas law and the relation between the temperature and the pressure in saturated condition (expressed by mean of a 2<sup>nd</sup> order polynomial).

$$P_{sat}(T_V(t)) = \frac{n(t) \cdot \bar{R} \cdot T_V(t)}{V_V} \quad (9)$$

$$P_{sat} = aT_V^2 + bT_V + c \quad (10)$$

The vapour temperature and thus the temperature of the interface for the upper film and the meniscus are determined by the following equation:

$$aT_V(t)^2 + \left( b - \frac{n(t) \cdot \bar{R}}{V} \right) \cdot T_V(t) + c = 0 \quad (11)$$

The meniscus is assumed to have a toric shape. The volume of the liquid films are neglected ( $V_{film}/V_V \approx 1\%$ ). The pressure is deduced from Equation (9).

## Sample – bubble Thermal coupling

The energy needed for the bubble growth is removed from the surrounding liquid and from the heated sample. The transient heat conduction problem within the heated bloc is solved and coupled with the energy balance governing the vaporisation of the lower liquid film.

The thermal coupling between the sample and the vaporisation of the lower liquid film is expressed using a heat transfer coefficient (12):

$$h_{inf}(r,t) = \left[ \frac{1}{h_{lim}} + \frac{\delta(r,t)}{\lambda_l} \right]^{-1} \quad (12)$$

The heat transfer coefficient  $h_{inf}(r,t)$  is used as a boundary condition to the no stationary heat conduction problem inside the heated block.

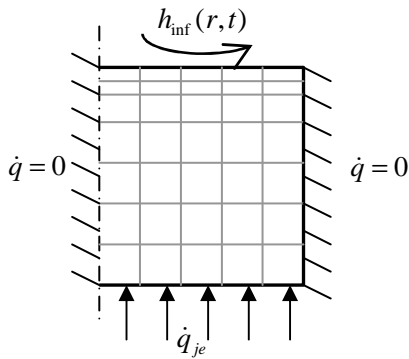


Fig 3: Sample mesh and boundary conditions

## Heat conduction equation inside the heated block

Considering the axi-symmetry of the problem, heat transfer within the heated bloc is determined by solving equation (13) (non stationary heat conduction equation in cylindrical coordinate):

$$\rho_s \cdot C_p \cdot \frac{\partial T}{\partial t} = \lambda_s \left( \frac{\partial^2 T}{\partial r^2} + \frac{1}{r} \frac{\partial T}{\partial r} + \frac{\partial^2 T}{\partial z^2} \right) \quad (13)$$

The lateral side of the bloc is assumed to be adiabatic. Considering the symmetry of the problem, heat flux along the

axis is set equal to zero. Desired heat flux can be imposed at the block bottom. The problem is closed with the heat transfer coefficient controlling the flux transferred to the fluid.

The scheme used to solve the aforementioned equations is presented in figure 4.

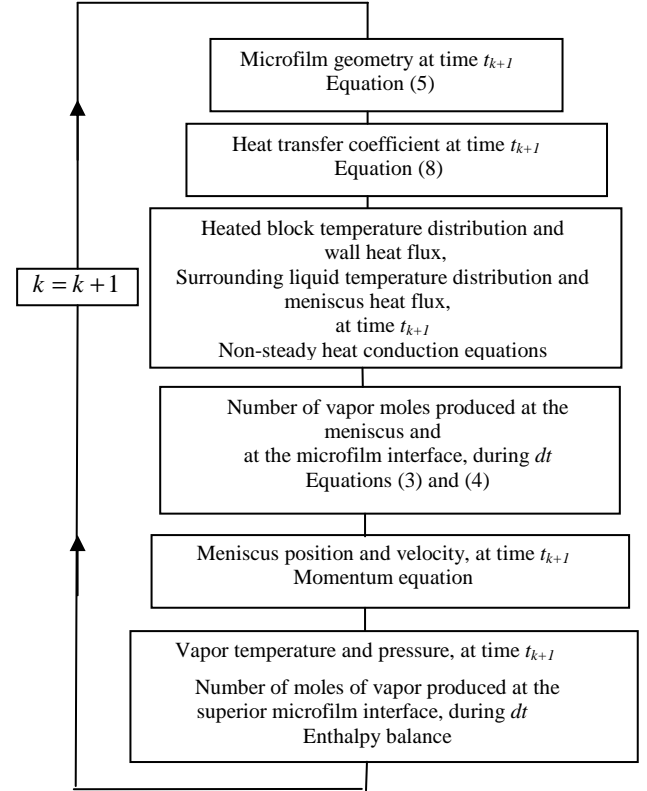


Fig. 4 : Scheme used for governing equations resolution

## Initial conditions

The calculation starts at the end of the spherical growth of bubble in the centre of the confinement place. The nucleation site is supposed to be located on the insulated confinement plate. The pressure inside the bubble is supposed to be equal to  $2\sigma/s$  (inertial effects are neglected). Vapour is supposed to be in saturated conditions. Heat flux required for the bubble growth is removed from the surrounding liquid. The temperature within the thermal boundary layer is assumed to vary linearly with the distance  $r$  (Figure 5). The thickness of the boundary layer is determined using energy balance.

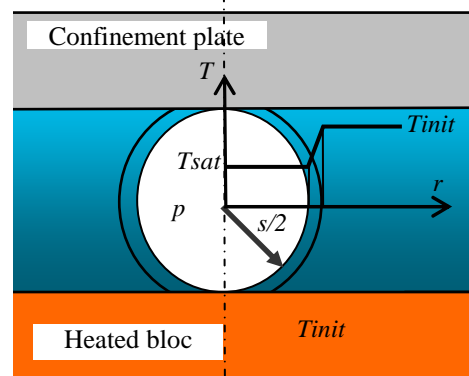


Fig. 5: Initial conditions

## NUMERICAL TREATMENT OF THE GOVERNING EQUATIONS

### Heat conduction equation inside the heated block

Equation (13) is solved using a finite difference scheme (alternate direction implicit method). The grid is uniform along the radial direction whereas a grading scheme is used in the vertical direction: cells are thinner near the wall where an important temperature gradient is expected. The program has been validated with different well known steady and unsteady solutions.

### Heat conduction in the liquid ring

Meniscus temperature is equal to vapour temperature (assumption 8). The domain meshed is so large that at the end of the bubble growth, thermal disturbance has not reached the domain end. Therefore, the related boundary condition is not of primal importance: it was chosen to set the temperature.

Due to the simplifications previously presented, the finite difference discretized non-stationary heat conduction equation is obtained from an energy balance over a control volume.

As the bubble grows, liquid distribution evolves. Therefore, the mesh is adapted at each time step in order to take the liquid shape evolution into account.

### Momentum equation

It is solved using fourth order Runge Kutta method. Implementation reliability is tested by solving simple second order differential equations having analytical solutions.

## RESULTS

The axi-symmetric model is applied to pentane bubble growth between a horizontal heated upward-facing disc (5mm depth and 30 mm diameter) and an unheated downward-facing disc placed parallel to the heated surface. The pressure of the system is 1bar. The influence of the gap size, the initial temperature of the system, the thermal effusivity of the heated wall and the kinetic limit of vaporisation are studied.

First of all, the spatial and the time evolution of the characteristic variables of the problem are studied for a reference condition: The bubble grows between the heated copper bloc and the insulating surface; the gap size is  $s=0.8\text{mm}$  ( $s/L_{cap}=0.5$ ); the initial superheat of the system (heated bloc and liquid) before onset of boiling is equal  $\Delta T_{sat_{init}}=20\text{K}$ . The accommodation coefficient used to determine the interfacial heat transfer coefficient at the interface is fixed to  $\alpha=0.02$ .

The growth rate of the bubble increases with time (Figure 9a). This tendency is due to the increase of the thickness of the liquid film  $\delta_0$  at the base of the travelling meniscus, and thus to the length of the liquid film between the bubble and the heated surface (in the present case, the modified Bond number  $Bo^*$  is smaller than 2. The thickness of the liquid film  $\delta_0$  at the base of the travelling meniscus is controlled by the capillary number. It increases with the increase of the growth rate of the bubble).

The heat flux transferred from the heated surface to the fluid depends on the depth of the liquid film. It becomes maximum near the triple line. Heat transfer coefficient is equal to the inverse of the interface thermal resistance at this location (Figure 6).

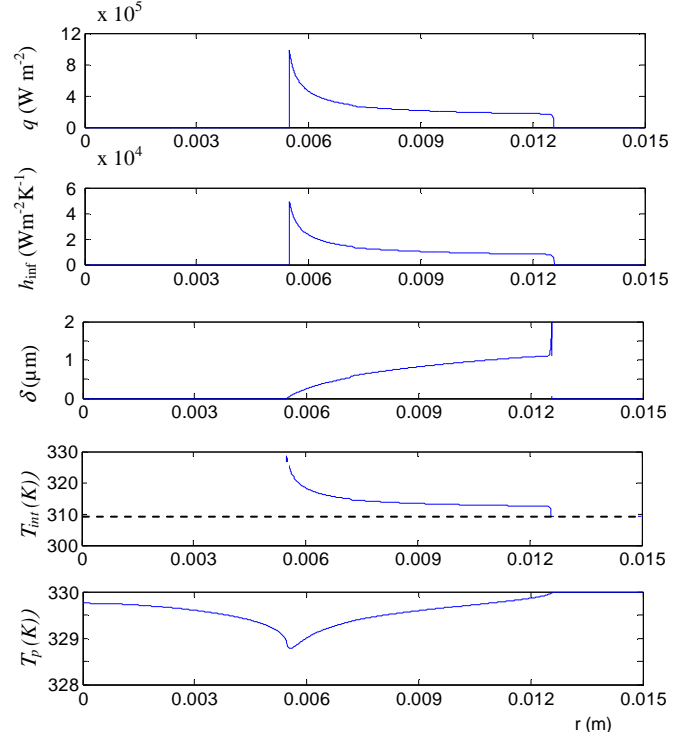


**Fig. 6:** Distribution of heat flux, heat transfer coefficient, depth of the liquid film, temperature of the interface and temperature of the heated surface as a function of the radius for a meniscus position  $r=13\text{ mm}$  ( $s=0.8\text{mm}$ ;  $\Delta T_{sat_{ONB}}=20\text{K}$ ; copper heater;  $\alpha=0.02$ )

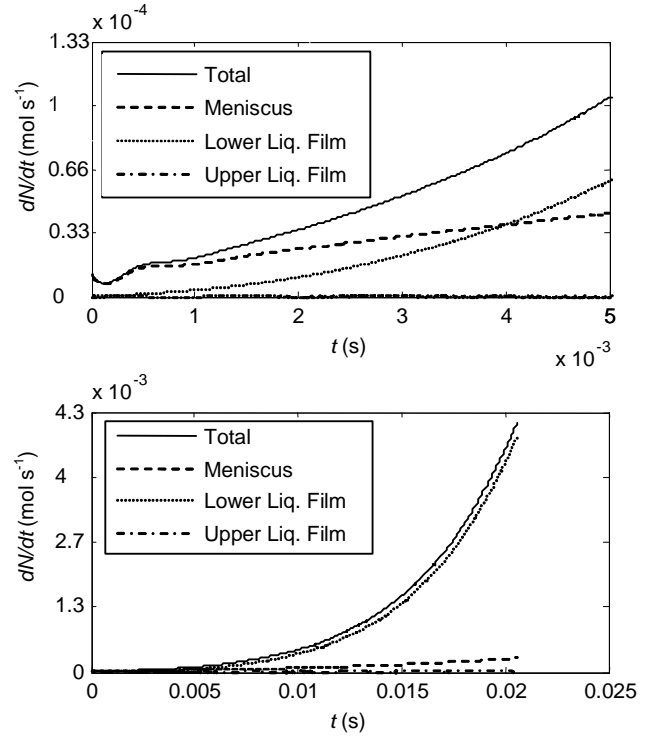


**Fig. 7:** Distribution of the time derivative of the vapour mole number from the meniscus, the lower and the upper liquid films as a function of time (a : early stages ; b entire cycle)

The vaporisation rate at the interface of the liquid film is very high and the thermal interface resistance have to be taken

into account. The interface superheat is enclosed between 4K at the base of the meniscus and 18.8K at the triple line (Figure 6). The vapour is mainly generated on the meniscus interface at the early stages of the bubble growth. The vapour production on the lower liquid film becomes rapidly higher than the other interfaces (Figure 7). The vapour flow-rate from the meniscus is affected by the pressure increase at the early stages of the bubble growth (figure 9.c) and the thermal boundary layer increase into the liquid. The vapour flow rate (vaporisation or condensation) on the upper liquid film is always negligible.

Because of the large diffusivity of the copper, the maximum temperature drop of the heated surface is about 1.2K at the triple line. The high growth rate of the bubble limits the depth of penetration of the cooling within the heated bloc. For the reference case, this length is about  $\delta_r \approx \sqrt{at} = 1.5\text{mm}$  (Figure 8). The heat condition imposed at the base of the liquid film rather corresponds to an imposed temperature than an imposed heat flux.

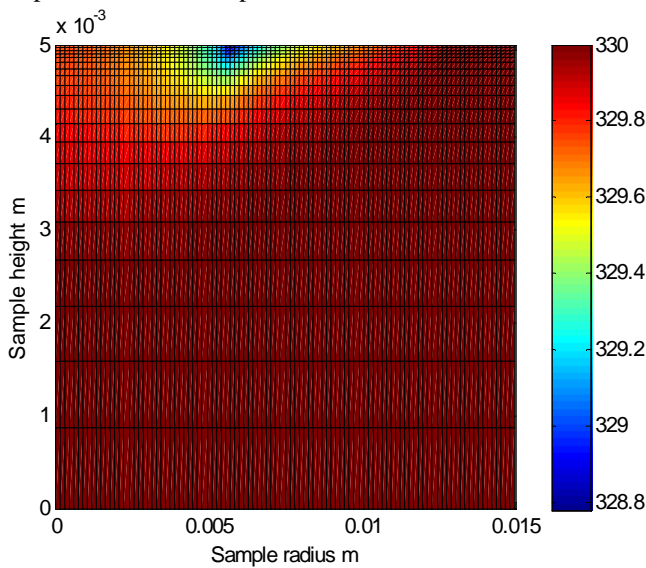


**Fig.8:** Distribution of the temperature within the heater ( $s=0.8\text{mm}$  ;  $\Delta T_{sat_{ONB}} = 20\text{K}$  ; copper heater)

The value of the accommodation coefficient affects the bubble growth when its value is lower than 0.02 (the bubble growth is directly controlled by the vapour production except at the early stage of the bubble growth) (Figure 9.a ; 9.c).

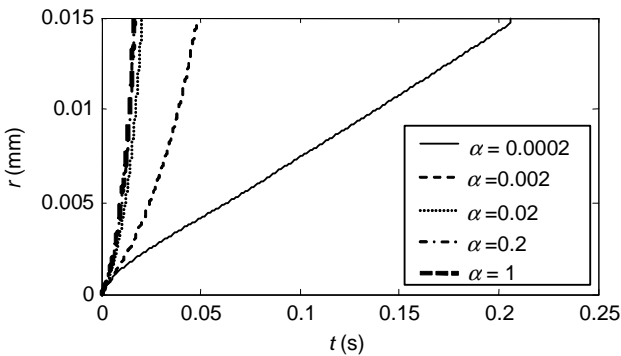


**Fig.9a :** Time evolution of the meniscus radius for different accommodation coefficient ( $s=0.8\text{mm}$  ;  $\Delta T_{sat_{ONB}} = 20\text{K}$  ; copper heater)

For higher values of  $\alpha$ , the friction forces play also an important role on the bubble growth and thus on the depth of the liquid film at the base of the bubble. The temperature drop at

the interface strongly depends on thermal interface resistance. It should be equal to the liquid superheat at the triple line for accommodation coefficient equal to unity. The time spatial discriminations are not high enough to describe it (Figure 9.b).

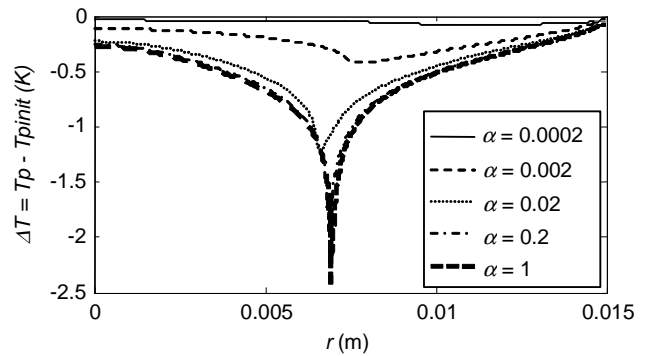


**Fig. 9b:** distribution of temperature drop of the heater surface when the meniscus reach the limit of the confinement space for different accommodation coefficient ( $s=0.8\text{mm}$  ;  $\Delta T_{sat_{ONB}} = 20\text{K}$  ; copper heater ;  $r_i = 0.015\text{m}$ )

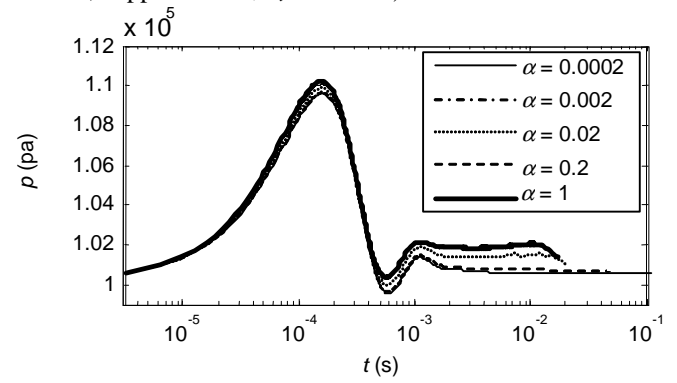


**Fig. 9c:** Time evolution of the vapour pressure for different accommodation coefficient ( $s=0.8\text{mm}$  ;  $\Delta T_{sat_{ONB}} = 20\text{K}$  ; copper heater)

The bubble growth duration doesn't vary linearly with the initial liquid superheat for different reasons (Figure 10.a). First of all because the depth of the liquid film at the base of the bubble, and thus the amount of liquid deposited on the heated surface, increase with the bubble growth rate increase. Next because the inertia forces (at the early stages) and the viscous forces are opposed to the bubble growth (Figure 10.c). And finally because the thermal effect that affects the surface temperature and thus the heat flux transferred to the fluid is all the more important since the growth rate is important (diffusion effect) (figure 10.b)

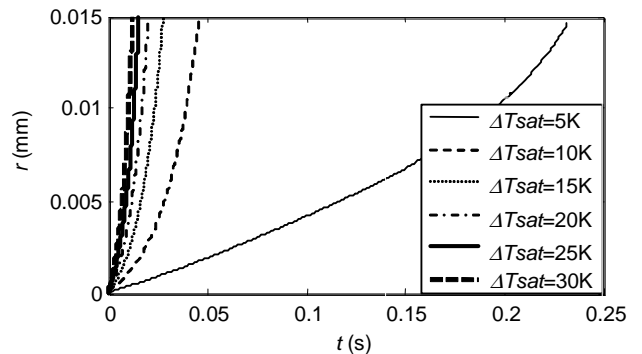


**Fig. 10a:** Time evolution of the meniscus radius for different system superheat at the onset of boiling ( $\alpha = 0.02$ ;  $s = 0.8\text{mm}$ ; copper heater)

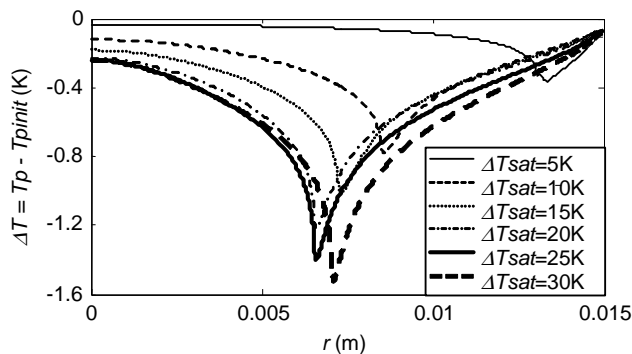


**Fig. 10b:** Distribution of temperature drop of the heater surface when the meniscus reach the limit of the confinement space for different system superheat at the onset of boiling ( $\alpha = 0.02$ ;  $s = 0.8\text{mm}$ ; copper heater;  $r_i = 0.015\text{m}$ )

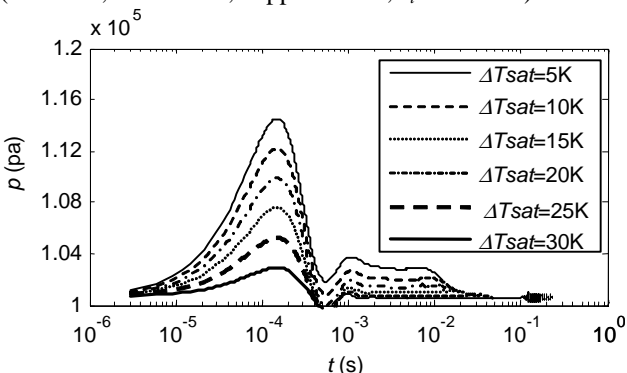


**Fig. 10c:** Time evolution of the vapour pressure for different system superheat at the onset of boiling ( $\alpha = 0.02$ ;  $s = 0.8\text{mm}$ ; copper heater)

The bubble growth rate duration is all the most small than the gap size is small (Figure 11a). The growth duration varies quasi linearly with the gap size for  $s > 0.1$ . The velocity effects on  $\delta_0$  are partially compensated by the capillary effects.  $\delta_0 = Cst.s.U^{0.41}$ . The increase of  $\delta$  with the increase of the gap size lead to the increase of the thermal resistance of the liquid film, and thus to the vaporisation process.

The viscous forces become significant and control the vapour growth when the gap size becomes too small ( $s < 0.2\text{mm}$ ) (Figure 11.c). The viscous forces depend on two effects: the velocity gradient (which increases with the bubble growth rate increase and gap size reduction); the size of the surface located under the liquid annulus. The significant reduction of this surface explains the reduction of the pressure at the end of the bubble growth.

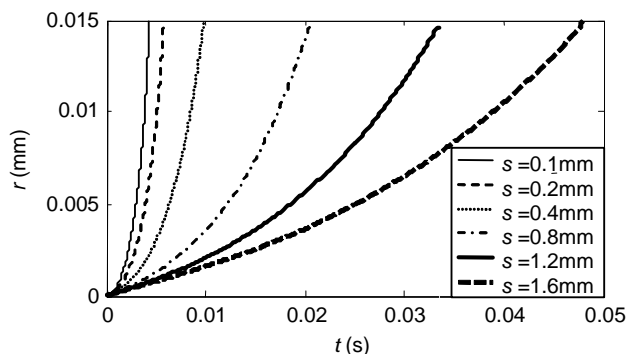


**Fig. 11a:** Time evolution of the meniscus radius for different confinement gap size ( $\alpha = 0.02$ ;  $\Delta T_{sat_{ONB}} = 20\text{K}$ ; copper heater)

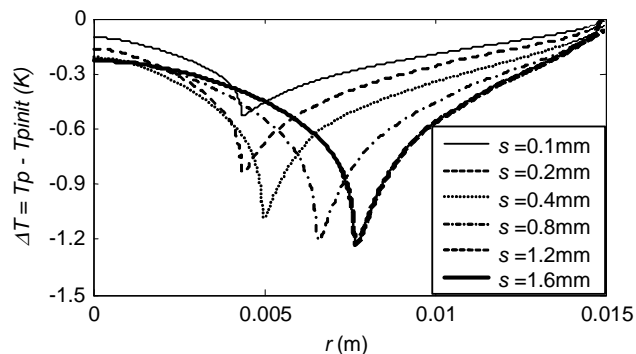


**Fig. 11b:** distribution of temperature drop of the heater surface when the meniscus reach the limit of the confinement space for different confinement gap sizes ( $\alpha = 0.02$ ;  $\Delta T_{sat_{ONB}} = 20\text{K}$ ; copper heater)

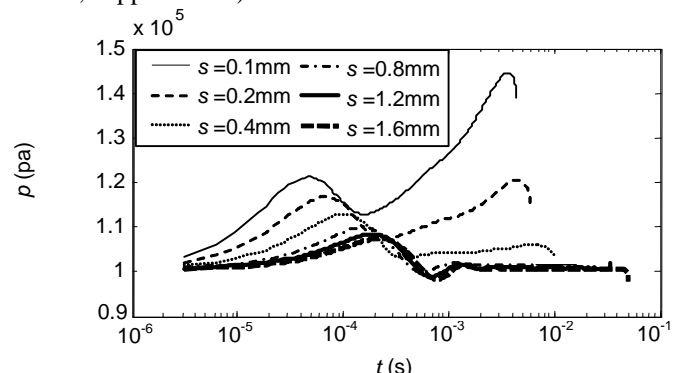


**Fig. 11c:** Time evolution of the vapour pressure for different confinement gap size ( $\alpha = 0.02$ ;  $\Delta T_{sat_{ONB}} = 20\text{K}$ ; copper heater)

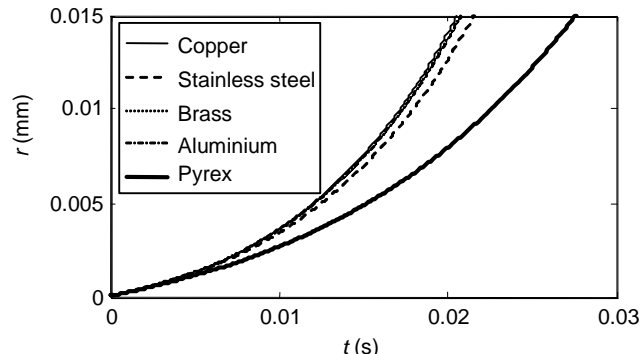


**Fig. 12a:** Time evolution of the meniscus radius for different heater blocs ( $\alpha = 0.02$ ;  $\Delta T_{sat_{ONB}} = 20\text{K}$ ;  $s = 0.8\text{mm}$ )

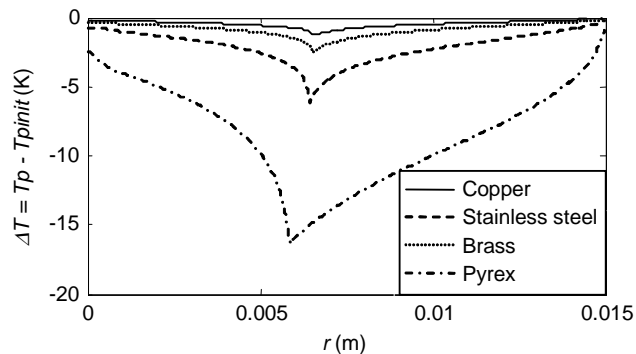


**Fig. 12b:** Distribution of temperature drop of the heater surface when the meniscus reach the limit of the confinement space for different heater blocs ( $\alpha = 0.02$ ;  $\Delta T_{sat_{ONB}} = 20\text{K}$ ;  $s = 0.8\text{mm}$ ;  $r_i = 0.015\text{m}$ )

The effect of the effusivity on the bubble growth is very limited except for low effusivity (figures 12a; 12b)). The effects of the thermal diffusivity appear on the distribution of temperature drop on the heater surface. The maximum temperature drop of the heated surface is about 1.2K using copper whereas it reaches 16K using Pyrex (figure 12b)

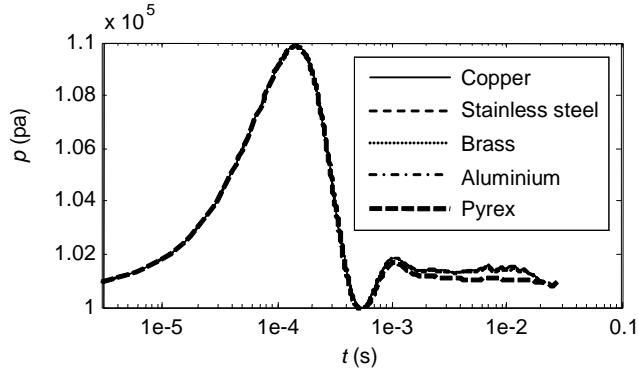


**Fig. 12c:** Time evolution of the vapour pressure for different accommodation coefficient ( $s=0.8\text{mm}$ ;  $\Delta T_{\text{sat ONB}} = 20\text{K}$ ; copper heater)

## CONCLUSION

An axi-symmetric two-phase flow model describing the growth of a single bubble squeezed between a horizontal heated upward-facing disc and an insulating surface placed parallel to the heated surface has been developed. The early results show that for high diffusive material, the heat condition imposed at the base of the liquid film look imposed temperature rather than imposed heat flux. The interface temperature of the heated liquid film is highly superheated.

## NOMENCLATURE

$Bo$	Bond number
$Bo^*$	Modified bond number
$Ca$	Capillary number
$h$	Heat transfer coefficient, $\text{W m}^{-2} \text{K}^{-1}$
$m$	Mass, kg
$\bar{M}$	Molar mass, $\text{kg mol}^{-1}$
$N$	mole number
$\dot{q}$	Heat flux, $\text{Wm}^{-2}$
$r$	Radial coordinate, m
$R$	Sample radius, m
$\bar{R}$	Ideal gas constant, $\text{J K}^{-1} \text{mol}^{-1}$
$s$	Confinement gap, m
$S$	Area, $\text{m}^2$
$t$	Time, s
$u$	Liquid velocity in the radial direction, $\text{m s}^{-1}$
$V$	Volume $\text{m}^3$
$z$	Vertical coordinate, m
$\alpha$	Accommodation coefficient
$\lambda$	Thermal conductivity, $\text{W m}^{-1} \text{K}^{-1}$
$\delta$	Layer thickness, m
$\Delta h_v$	Latent heat, $\text{J kg}^{-1}$
$\mu$	Dynamic viscosity, Pa s
$\nu$	Viscosity, $\text{m}^2 \text{s}^{-1}$
$\rho$	Density, $\text{kg m}^{-3}$
$\sigma$	Surface tension, Nm

Subscripts, superscripts

0 Initial

i	Meniscus base
inf	Inferior microfilm
je	Joule effect
k	$k^{\text{th}}$ iteration 1,2 Bubble main radii
l	Liquid
lim	Limit
men	Meniscus
s	Sample
sat	Saturated
v	Vapor
wall	Sample superior wall

## REFERENCES

1. B. Stutz, M. Lallemand, F. Raimbault, J.C. Passos, Nucleate and transition boiling in narrow horizontal spaces, *Heat and Mass Transfer*, DOI 10.1007/s00231-007-0325-9 7 p., 2007.
2. Y. Katto, S. Yokoya, Experimental study of nucleate pool-boiling in case of making interference-plate approach to the heating surface, *Proc. 3rd Int. J. Heat Transfer Conf*, Chicago: 219-227, 1966.
3. Y. Katto, S. Yokoya, K. Terakoa K. Nucleate and transition boiling in a narrow space between two horizontal parallel disk-surfaces, *Bull. JSME* 20: 638-643, 1977.
4. J.C. Passos, E.L. da Silva and L.F.B. Possamai, Visualization of FC72 Confined Nucleate Boiling, *Experimental Thermal and Fluid Science*, vol. 30, pp. 1-7, 2005.
5. E.M. Cardoso, B. Stutz, M. Lallemand, J.C. Passos, Effect of confinement on FC-72 and FC-87 nucleate boiling, *ECI International Conference on Boiling Heat Transfer*, Spoleto, 7-12 May 2006, 8p
6. Passos J. C., Hirata F. R., Possamai L. F. B., Balsamo M., Misale M.. (2004) Confined boiling of FC72 and FC87 on a downward facing heating copper disk, *Int. J. Heat Fluid Flow* 25: 313-319,
7. Lallemand M., Bonjour J., Gentile D., Boulanger F. (1998), The physical mechanisms involved in the boiling of mixtures in narrow spaces, *Int Heat Transfer Conference*, Kyongju – Korea: 515-519
8. B. Stutz, V. Tormen, Nucleate and transition boiling in inclined narrow spaces, *Micro/Nanoscale Heat Transfer International Conference*, January 6-9, Taiwan, 10p. 2008.
9. Y. Katto, M. Shoji, Principal mechanism of micro-liquid-layer formation on a solid surface with a growing bubble in nucleate boiling. *Int. J. Heat Mass Transfer*, 13(1969) 1299-1311
10. K. Moriyama, A. Inoue, Thickness of the Liquid Film Formed by a Growing Bubble in a Narrow Gap Between Two Horizontal Plates, *J. Heat Transfer*, 118 (1996) 132-139.
11. J.R. Thome, V. Dupont, A.M. Jacobi, Heat transfer model for evaporation in microchannels – Part I : presentation of the model, *Int. J. Heat and Mass Transfer* 47 (2004) 3387-3401